

# PARAMETRIZATION OF A NONLOCAL CHIRAL QUARK MODEL IN THE INSTANTANEOUS THREE-FLAVOR CASE. BASIC FORMULAS AND TABLES

*H. Grigorian*<sup>1</sup>

Institut für Physik, Universität Rostock, Rostock, Germany

We describe the basic formulation of the parametrization scheme for the instantaneous nonlocal chiral quark model in the three-flavor case. We choose to discuss the Gaussian, Lorentzian-type, Woods–Saxon and sharp cutoff (NJL) functional forms of the momentum dependence for the form factor of the separable interaction. The four parameters: light and strange quark masses, coupling strength ( $G_S$ ) and range of the interaction ( $\Lambda$ ) have been fixed by the same phenomenological inputs: pion and kaon masses, pion decay constant and light quark mass in vacuum. The Woods–Saxon and Lorentzian-type form factors are suitable for an interpolation between sharp cutoff and soft momentum dependence. Results are tabulated for applications in models of hadron structure and quark matter at finite temperatures and chemical potentials where separable models have been proven successfully.

Дано описание основной формулировки схемы параметризации для одновременной нелокальной киральной кварковой модели в трехфлейворном случае. Для обсуждения выбрана импульсная зависимость формфактора сепарабельного взаимодействия в виде функций Гаусса, Лоренца, Вудса–Саксона, а также простое обрезание (НИЛ). Четыре параметра — массы легкого и странного кварков, константа взаимодействия ( $G_S$ ) и размер области взаимодействия ( $\Lambda$ ) — были фиксированы при помощи одних и тех же феноменологических данных: масс пиона и каона, константы распада пиона и массы легкого кварка в вакууме. Формфакторы Вудса–Саксона и Лоренца удобны для интерполяции между простым обрезанием и мягкой импульсной зависимостью. Результаты затабулированы для использования в моделях структуры адронов и кварковой материи при конечных температурах и химических потенциалах, где сепарабельные модели успешно применялись.

PACS: 04.40.Dg, 12.38.Mh, 26.60.+c

## INTRODUCTION

The phase diagram of Quantum Chromodynamics (QCD) is investigated in large-scale lattice gauge theory simulations [1] and in heavy-ion collision experiments at the SPS CERN and RHIC (Brookhaven) [2], where the approximately baryon-free region at finite temperatures is accessible and consensus about the critical temperature for the occurrence of a strongly

---

<sup>1</sup>Permanent address: Department of Physics, Yerevan State University, 375047 Yerevan, Armenia.

correlated quark–gluon plasma phase (sQGP) is developing. The region of low temperatures and high baryon densities, however, which is interesting for the astrophysics of compact stars, is not yet accessible to lattice QCD studies and heavy-ion collision experiments such as the CBM experiment at FAIR (Darmstadt) are still in preparation [3]. The most stringent of the presently available constraints on the EoS of superdense hadronic matter from compact stars and heavy-ion collisions have recently been discussed in Ref. [4] and may form the basis for future systematic investigations of the compatibility of dense quark matter models with those phenomenological constraints. Therefore, the question arises for appropriate models describing the nonperturbative properties of strongly interacting matter such as dynamical chiral symmetry breaking and hadronic bound state formation in the vacuum and at finite temperatures and densities.

The Nambu–Jona-Lasinio (NJL) model has been proven very useful for providing results to this question within a simple, but microscopic formulation, mostly on the mean-field level, see [5]. The state of the art phase diagrams of neutral quark matter for compact star applications has recently been obtained in [6–9], where references to other approaches can be also found. One of the shortcomings of the NJL model is the absence of confinement, the other is its nonrenormalizability. It is customary to speak of the NJL model in its form with a cutoff regularization, where physical observables can be defined and calculated. The cutoff in momentum space, however, defines a range of the interaction and makes the NJL model nonlocal. It has been suggested that the cutoff-regularized NJL model can be considered as a limiting case of a more general formulation of nonlocal chiral quark models using separable interactions [10]. In this form one can even make contact with the Dyson–Schwinger equation approach to QCD by defining a separable representation of the effective gluon propagator [11], or to the instanton liquid model, see [12].

We have made extensive use of the parametrization given in [10], for studies of quark matter phases in compact stars [13, 14], where the role of the smoothness of the momentum dependence for the quark–hadron phase transition and compact star structure has been explored. These investigations have been also used in simulations of hybrid star cooling [15, 16], which can be selective for the choice of the equation of state (EoS) of quark matter by comparing to observational data for the surface temperature and the age of compact stars. As a result of these studies, color superconducting phases with small gaps of the order of  $10 \text{ keV} - 1 \text{ MeV}$  appear to be favorable for the cooling phenomenology. A prominent candidate, the color-spin-locking (CSL) phase, has been investigated in more detail within the NJL model with satisfactory results [17]. However, its generalization to form factors with a smooth momentum dependence revealed a severe sensitivity resulting in variations of the CSL gaps over four orders of magnitude [18].

Unfortunately, with the NJL parametrization given in [10] it was not possible to reproduce results with NJL parametrizations given in [5] and used, e.g., in Refs. [6, 7, 17]. Therefore, in the present work a new parametrization of the model presented in Ref. [10] is performed with a special emphasis on reproducing NJL parametrizations given in [5] in the limiting case of a sharp cutoff form factor. We also take into account the strangeness degree of freedom and consider Lorentzian-type form factor models, where the form of the momentum dependence for the quark–quark interaction can be varied parametrically, thus being most suitable for a quantitative analysis of the phase diagram and high-density EoS under the above-mentioned constraints from compact star and heavy-ion collision phenomenology.

## 1. BASIC FORMULATION

We consider a nonlocal chiral quark model with separable quark–antiquark interaction in the color singlet scalar/pseudoscalar isovector channel [19], where the form factors are given in the instantaneous approximation, in the same way as it was suggested in [10].

The Lagrangian density of the quark model is given by ( $i, j = u, d, s$ )

$$\mathcal{L} = \bar{q}_i(i\gamma_\mu\partial^\mu - m_{i,0})q_i + G_S \sum_{a=0}^8 [(\bar{q}_i\tilde{g}(x)\lambda_{ij}^a q_j)^2 + (\bar{q}_i(i\tilde{g}(x)\gamma_5)\lambda_{ij}^a q_j)^2], \quad (1)$$

where indices occurring twice are to be summed over and the form factor  $\tilde{g}(x)$  for the nonlocal current–current coupling has been introduced. Here,  $m_0 = m_{u,0} = m_{d,0}$  and  $m_{s,0}$  are the current quark masses of the light and strange flavors, respectively,  $\lambda_{ij}^a$  are the Gell-Mann matrices of the  $SU(3)$  flavor group and  $\gamma_\mu, \gamma_5$  are the Dirac matrices.

The nonlocality of the current–current interaction in the quark–antiquark ( $q\bar{q}$ ) channel is implemented in the separable approximation via the same form factor functions for all colors and flavors. In our calculations we use the Gaussian ( $G$ ), Lorentzian ( $L$ ), Woods–Saxon ( $WS$ ) and cutoff (NJL) form factors in the momentum space defined as (see Ref. [10])

$$\begin{aligned} g_G(p) &= \exp(-p^2/\Lambda_G^2), \\ g_L(p) &= [1 + (p/\Lambda_L)^{2\alpha}]^{-1}, \\ g_{WS}(p) &= [1 + \exp(-\alpha)]/\{1 + \exp[\alpha(p^2/\Lambda_{WS}^2 - 1)]\}, \\ g_{NJL}(p) &= \theta(1 - p/\Lambda_{NJL}). \end{aligned}$$

The form factors can be introduced in a manifestly covariant way (see [19]), but besides technical complications at finite  $T$  and  $\mu$ , where Matsubara summations have to be performed numerically, it is not a priori obvious that such a formulation shall be superior to an instantaneous approximation (3D) which could be justified as a separable representation of a Coulomb-gauge potential model [20].

Typically, three-flavor NJL type models use the 't Hooft determinant interaction that induces a  $U_A(1)$  symmetry breaking in the pseudoscalar–isoscalar meson sector, which can be adjusted such that the  $\eta$ – $\eta'$  mass difference is described. In the present approach, this term is neglected using the motivation given in [7], so that the flavor sectors decouple in the mean-field approximation.

The dynamical quark mass functions are then given by  $M_i(p) = m_{i,0} + \phi_i g(p)$ , where the chiral gaps fulfill the gap equations

$$\phi_i = 4G_S \frac{N_c}{\pi^2} \int dp p^2 g(p) \frac{M_i(p)}{E_i(p)}, \quad (2)$$

corresponding to minima of the thermodynamic potential with respect to variations of the order parameters  $\phi_i$ , and the quark dispersion relations are  $E_i(p) = \sqrt{p^2 + M_i^2(p)}$ .

The basic set of equations should be chosen to fix the parameters included in the model, which are the current masses, coupling constant and cutoff parameter ( $m_0, m_{s,0}, G_S$  and  $\Lambda$ ).

In order to do that, we use the properties of bound states of quarks in the vacuum given by the pion decay constant  $f_\pi = 92.4$  MeV, the masses of the pion  $M_\pi = 135$  MeV and the

kaon  $M_K = 494$  MeV, and either the constituent quark mass  $M(p=0) = m_0 + \phi_u$  or the chiral condensate of light quarks, defined as

$$\langle u\bar{u} \rangle_0 = -\frac{N_c}{\pi^2} \int dp p^2 \frac{M_u(p) - m_0}{E_u(p)}, \quad (3)$$

with a phenomenological value from QCD sum rules [21] of  $190 \leq -\langle u\bar{u} \rangle_0^{1/3} \leq 260$  MeV. The chiral condensate generally is not properly defined in the case of nonlocal interactions. The subtraction of the  $m_0$  term has been included to make the integral convergent.

The pion decay constant can be expressed in the form

$$f_\pi = \frac{3}{2\pi^2} \frac{g_{\pi q\bar{q}}}{\pi^2} \int dp p^2 g(p) \frac{M_u(p)}{E_u(p)(E_u(p)^2 - M_\pi^2/4)}, \quad (4)$$

where the pion wave function renormalization factor  $g_{\pi q\bar{q}}$  is

$$g_{\pi q\bar{q}}^{-2} = \frac{3}{2\pi^2} \int dp p^2 g^2(p) \frac{E_u(p)}{(E_u(p)^2 - M_\pi^2/4)^2}.$$

The masses of pion and kaon are obtained from a direct generalization of the well-known NJL model [22, 23] by introducing form factors with the momentum space integration and replacing constituent quark masses by the momentum-dependent mass functions  $M(p)$

$$M_\pi = \left[ \left( \frac{1}{2G_S} - 2I_u^{(1)} \right) / I_{uu}^{(2)} \right]^{1/2}, \quad (5)$$

$$M_K = \left[ \left( \frac{1}{2G_S} - (I_u^{(1)} + I_s^{(1)}) \right) / I_{us}^{(2)} \right]^{1/2}. \quad (6)$$

In these mass formulae, the following abbreviations for integrals have been used

$$\begin{aligned} I_i^{(1)} &= \frac{3}{\pi^2} \int dp p^2 g^2(p) \frac{1}{E_i(p)}, \\ I_{uu}^{(2)} &= \frac{3}{2\pi^2} \int dp p^2 \frac{g^2(p)}{E_u(p)(E_u(p)^2 - M_\pi^2/4)}, \\ I_{us}^{(2)} &= \frac{3}{\pi^2} \int dp p^2 g^2(p) \frac{E_u(p) + E_s(p)}{E_u(p)E_s(p)[(E_u(p) + E_s(p))^2 - M_K^2]}. \end{aligned} \quad (7)$$

We can use these notations to give an estimate of the validity of low-energy theorems for this nonlocal generalization of the NJL model. To this end, we rewrite Eq. (4) for  $f_\pi$  and  $g_{\pi q\bar{q}}$  as

$$f_\pi = g_{\pi q\bar{q}} (\phi_u I_{uu}^{(2)} + m_0 \langle g^{-1}(p) \rangle^{(2)}), \quad (8)$$

$$g_{\pi q\bar{q}}^{-2} \approx I_{uu}^{(2)} + M_\pi^2/4 \langle E_u^{-2}(p) \rangle^{(2)}, \quad (9)$$

where the mean values of a distribution  $F(p)$  are defined using the integral  $I_{uu}^{(2)}$  as an operator:  $\langle F(p) \rangle^{(2)} = I_{uu}^{(2)} [F(p)]$ . To leading order in an expansion at the chiral limit ( $m_0 \rightarrow 0$ ,  $M_\pi \rightarrow 0$ ) one obtains the Goldberger-Treiman relation

$$f_\pi g_{\pi q\bar{q}} = \phi_u. \quad (10)$$

Rewriting gap equation (2) for the light flavor as

$$\phi_u[1 - 4G_S I_u^{(1)}] = -m_0 \langle u\bar{u} \rangle_0 4G_S, \quad (11)$$

and the pion mass formula (5) as

$$M_\pi^2 = \frac{1}{2G_S} \left(1 - 4G_S I_u^{(1)}\right) / I_{uu}^{(2)}, \quad (12)$$

by combining (12) with (11), (10) and (8) in leading order we obtain the Gell-Mann–Oakes–Renner relation (GMOR)

$$M_\pi^2 f_\pi^2 = -2m_0 \langle u\bar{u} \rangle_0. \quad (13)$$

As an indicator of the validity of this low-energy theorem we will show the GMOR value for the light current quark mass

$$m_0^{\text{GMOR}} = -\frac{M_\pi^2 f_\pi^2}{2\langle u\bar{u} \rangle_0} \quad (14)$$

together with the result of the parametrization of  $m_0$ .

Since we have no 't Hooft term, there is no mixing of flavor sectors, and one can consider the light quark sector independently of the strange one. The equation for the kaon mass fixes the strange quark's current mass  $m_{s,0}$ , whereby a self-consistent solution of the strange quark gap equation is implied.

## 2. RESULTS

In the present parametrization scheme the gap equation plays a special role. Although the gap is not an observable quantity, we will use it as a phenomenological input instead of the condensate, which in some cases does not fulfill the phenomenological constraints. Moreover, for each form-factor model there is some minimal value of  $G_S \Lambda^2$  for which the condensate has a minimum: for the Gaussian model it is 7.376, for the Lorentzian model with  $\alpha = 2$  it is 3.795, and for  $\alpha = 10$  it is 2.825. For the NJL model this minimal value is 2.588. The corresponding values of the condensate are given in Table 6. These values for the finite current masses are shifted to the left as is shown in Fig. 1 and for them the parameter sets are fixed (see Table 6). When the condensate is chosen there are two possible values of  $G_S \Lambda^2$  (the lower and higher branches) for which one can fix the parameters of the model. We show that the constraint on the condensate from QCD sum rules [21] with an upper limit at 260 MeV can be fulfilled only for values of  $\alpha$  exceeding 3–5 for both Lorentzian and Woods–Saxon form-factor models. For the particular choice of  $-\langle u\bar{u} \rangle^{1/3} = 280$  and 260 MeV we fixed the parameters for both branches of solutions (see Tables 7–11).

In order to obtain the parameter sets, we choose three values for the non-observable value of the constituent quark mass  $M(p=0) = 330, 335, 367.5, 380,$  and 400 MeV. The values are taken such that the mass  $3M(p=0)$  is larger than the mass of the nucleon as a bound state of three quarks. The results of the parametrizations are given in Tables 1–5.

In Fig. 1, the dependence of the chiral condensate is shown as a function of  $G_S \Lambda^2$  for different form factors in the chiral limit band for an appropriate choice of the current mass  $\sim 0.01 \Lambda$ . It is shown that the minimal possible value of the condensate varies from one

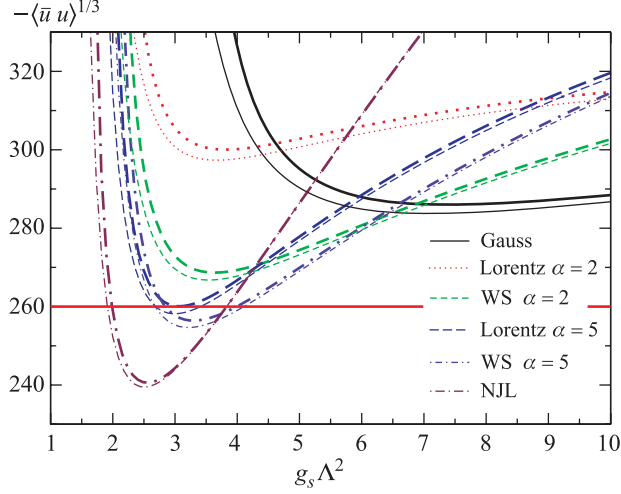


Fig. 1. The dependence of the chiral condensate  $-\langle\bar{u}u\rangle^{1/3}$  on the choice of the coupling constant in the chiral limit (thick lines) and for finite current mass of the light quark  $m_0 \simeq 0.01 \Lambda$  (thin lines) for different form-factor models. The plot demonstrates that not for all cases the phenomenological constraint for the value of the condensate from QCD sum rules [21] with an upper limit at 260 MeV can be fulfilled

Table 1. Parameter sets for the chiral quark model with Gaussian, Woods–Saxon and Lorentzian form factors for different values of the  $\alpha$  parameter (including cutoff), when  $M(p=0) = 330$  MeV

$\alpha$	$-\langle\bar{u}\bar{u}\rangle^{1/3}$ , MeV	$m_0$ , MeV	$m_0^{\text{GMOR}}$ , MeV	$m_{s,0}$ , MeV	$G_S \Lambda^2$	$\phi_{u,d}$ , MeV	$\phi_s$ , MeV	$\Lambda$ , MeV
$G$	329.505	2.17720	2.17482	84.4205	3.88079	327.823	661.678	891.044
WS 2	287.231	3.26230	3.28314	118.698	2.53185	326.738	567.983	681.824
5	264.453	4.16354	4.20674	143.118	2.59911	325.836	502.023	680.003
10	253.498	4.71893	4.77597	157.138	2.39385	325.281	467.880	653.577
$L$ 2	320.280	2.36668	2.36805	86.3960	2.57512	327.633	613.944	703.442
5	266.053	4.09091	4.13132	139.122	2.49292	325.909	500.191	666.553
10	253.699	4.70805	4.76458	156.362	2.35908	325.292	467.132	649.168
$\infty$	244.135	5.27697	5.34681	171.210	2.17576	324.723	438.791	629.540

form-factor model to another, and only in the NJL model the appropriate values of condensate in the range of QCD sum rule values ( $230 \pm 10$ ) MeV can be reached. Figures 2 and 3 show the gap function and the diagonal elements of the separable interaction for different form factors in order to demonstrate the systematics of the changes related to the degree of the softening given by the parameter  $\alpha$  in the Lorentzian functions.

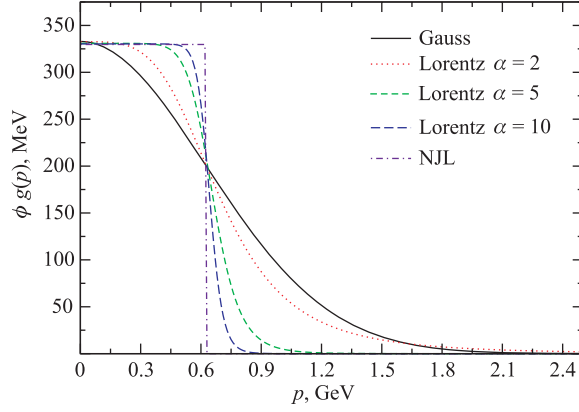


Fig. 2. The gap functions of light quarks for different form-factor models. The present parameter set is taken from Table 2

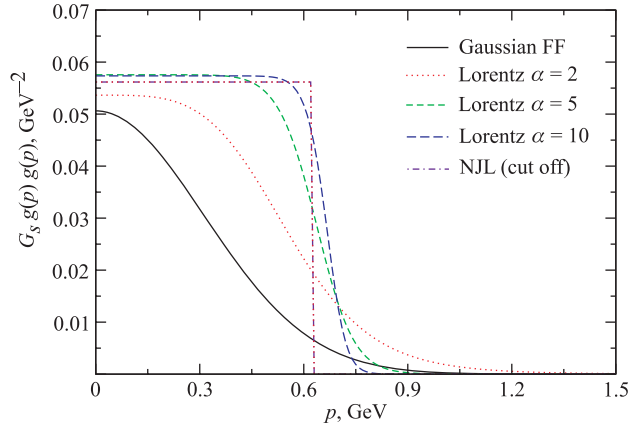


Fig. 3. The diagonal elements of the separable interaction  $G_S g(p)g(p)$  for different form-factor models. The results for the parameter set are given in Table 2

Table 2. Parameter sets for the chiral quark model with Gaussian, Woods–Saxon and Lorentzian form factors for different values of the  $\alpha$  parameter (including cutoff), when  $M(p = 0) = 335$  MeV

$\alpha$	$-\langle u\bar{u} \rangle^{1/3}$ , MeV	$m_0$ , MeV	$m_{s,0}$ , MeV	$G_S \Lambda^2$	$\phi_{u,d}$ , MeV	$\phi_s$ , MeV	$\Lambda$ , MeV
$G$	327.587	2.21473	85.3586	3.90437	332.785	664.996	878.215
WS 2	285.950	3.30539	119.481	2.55036	331.695	570.557	673.959
5	263.581	4.20424	143.560	2.62025	330.796	504.505	673.796
10	252.796	4.75777	157.365	2.41420	330.242	470.371	648.407
$L$ 2	319.000	2.39420	86.9114	2.59304	332.606	617.354	695.289
5	265.280	4.12606	139.418	2.51348	330.874	502.838	660.803
10	253.019	4.74558	156.553	2.37921	330.254	469.656	644.106
$\infty$	243.515	5.31583	171.300	2.19469	329.684	441.236	625.071

**Table 3. Parameter sets for the chiral quark model with Gaussian, Woods–Saxon and Lorentzian form factors for different values of the  $\alpha$  parameter (including cutoff), when  $M(p = 0) = 367.5$  MeV**

$\alpha$	$-\langle u\bar{u}\rangle^{1/3}$ , MeV	$m_0$ , MeV	$m_{s,0}$ , MeV	$G_S\Lambda^2$	$\phi_{u,d}$ , MeV	$\phi_s$ , MeV	$\Lambda$ , MeV
$G$	317.279	2.43126	90.5456	4.06161	365.069	687.275	808.486
WS 2	279.325	3.54048	123.328	2.67284	363.960	588.701	631.752
5	259.333	4.41036	145.100	2.75916	363.090	522.373	641.089
10	249.556	4.93983	157.470	2.54737	362.560	488.449	621.664
$L$ 2	312.381	2.54557	89.4547	2.71147	364.954	640.464	651.022
5	261.615	4.29837	140.125	2.64838	363.202	521.702	630.566
10	249.906	4.92671	156.442	2.51088	362.573	487.938	617.968
$\infty$	240.772	5.49540	170.417	2.31825	362.005	459.190	602.472

**Table 4. Parameter sets for the chiral quark model with Gaussian, Woods–Saxon and Lorentzian form factors for different values of the  $\alpha$  parameter (including cutoff), when  $M(p = 0) = 380$  MeV**

$\alpha$	$-\langle u\bar{u}\rangle^{1/3}$ , MeV	$m_0$ , MeV	$m_{s,0}$ , MeV	$G_S\Lambda^2$	$\phi_{u,d}$ , MeV	$\phi_s$ , MeV	$\Lambda$ , MeV
$G$	314.115	2.50324	92.1716	4.12364	377.497	696.149	786.678
WS 2	277.402	3.61367	124.331	2.72075	376.386	596.248	618.773
5	258.214	4.46967	145.205	2.81307	375.530	529.931	631.281
10	248.787	4.99173	157.022	2.59883	375.008	496.137	613.860
$L$ 2	310.457	2.59269	90.1287	2.75775	377.407	649.735	637.183
5	260.698	4.34314	139.962	2.70064	375.657	529.610	621.523
10	249.185	4.97096	155.921	2.56172	375.029	495.699	610.359
$\infty$	240.184	5.54297	169.559	2.36582	374.457	466.894	596.112

**Table 5. Parameter sets for the chiral quark model with Gaussian, Woods–Saxon and Lorentzian form factors for different values of the  $\alpha$  parameter (including cutoff), when  $M(p = 0) = 400$  MeV**

$\alpha$	$-\langle u\bar{u}\rangle^{1/3}$ , MeV	$m_0$ , MeV	$m_{s,0}$ , MeV	$G_S\Lambda^2$	$\phi_{u,d}$ , MeV	$\phi_s$ , MeV	$\Lambda$ , MeV
$G$	309.756	2.60719	94.4251	4.22432	397.393	710.653	756.140
WS 2	274.869	3.71199	125.506	2.79810	396.288	608.881	600.815
5	256.870	4.53517	144.962	2.89964	395.465	542.673	617.969
10	247.969	5.03928	155.906	2.68120	394.961	509.126	603.493
$L$ 2	307.917	2.65479	90.9372	2.83241	397.345	664.942	617.801
5	259.652	4.39512	139.341	2.78448	395.605	542.876	609.265
10	248.440	5.01137	154.700	2.64310	394.989	508.802	600.271
$\infty$	239.649	5.58218	167.771	2.44178	394.418	479.964	587.922



**Table 6. Parameter sets for the chiral quark model with Gaussian, Woods–Saxon and Lorentzian form factors for different values of the  $\alpha$  parameter, when  $-\langle u\bar{u}\rangle^{1/3}$  has its possible minimal value at chiral limit**

$\alpha$	$-\langle u\bar{u}\rangle^{1/3}$ , MeV	$m_0$ , MeV	$m_0^{\text{GMOR}}$ , MeV	$m_{s,0}$ , MeV	$G_S\Lambda^2$	$\phi_{u,d}$ , MeV	$\phi_s$ , MeV	$\Lambda$ , MeV
<i>G</i>	286.005	3.2971	3.3255	103.92	6.0252	733.24	987.97	548.85
WS 2	268.670	3.9696	4.0116	126.50	3.1643	489.09	674.48	546.23
5	256.425	4.5602	4.6142	144.72	2.9375	404.17	548.46	612.92
6	254.049	4.6875	4.7449	148.46	2.8288	393.39	530.26	615.00
7	252.221	4.7859	4.8488	151.37	2.7472	386.39	517.64	615.26
8	250.792	4.8765	4.9323	153.66	2.6857	381.60	508.55	614.82
9	249.655	4.9418	5.0000	155.49	2.6391	378.34	501.87	614.09
10	248.734	4.9959	5.0557	156.98	2.6030	376.01	496.77	613.28
12	247.344	5.0798	5.1415	159.23	2.5510	373.00	489.59	611.75
15	245.954	5.1659	5.2290	161.48	2.5019	370.57	482.97	609.89
20	244.575	5.2543	5.3181	163.72	2.4557	368.66	476.87	607.78
30	243.215	5.3318	5.4076	165.92	2.4123	367.29	471.30	605.46
40	242.545	5.3772	5.4526	167.01	2.3914	366.72	468.67	604.26
50	242.147	5.4046	5.4795	167.66	2.3791	366.43	467.13	603.53
<i>L</i> 2	300.991	2.8362	2.8531	91.830	3.2486	506.47	754.06	548.54
5	260.090	4.3692	4.4219	139.68	2.7448	386.17	536.51	614.76
6	256.288	4.5718	4.6218	145.31	2.6820	380.48	521.05	615.01
7	253.707	4.7101	4.7641	149.24	2.6358	377.05	510.78	614.46
8	251.844	4.8138	4.8706	152.13	2.6003	374.77	503.46	613.69
9	250.438	4.8945	4.9532	154.33	2.5722	373.18	498.01	612.88
10	249.341	4.9589	5.0190	156.07	2.5494	372.01	493.78	612.10
12	247.740	5.0549	5.1166	158.62	2.5147	370.43	487.68	610.74
15	246.195	5.1505	5.2135	161.10	2.4793	369.05	481.86	609.13
20	244.705	5.2459	5.3096	163.51	2.4433	367.88	476.31	607.30
30	243.272	5.3282	5.4039	165.83	2.4070	366.97	471.08	605.22
40	242.577	5.3752	5.4505	166.96	2.3884	366.55	468.55	604.12
50	242.167	5.4033	5.4782	167.62	2.3772	366.32	467.06	603.44

## CONCLUSIONS

We have presented parametrizations of nonlocal chiral quark models with instantaneous separable interactions defined by momentum-dependent form factors which interpolate between the soft Gaussian type and the hard cutoff (NJL) in tabulated form. The introduction of a Lorentzian and/or Woods–Saxon-type function with an additional parameter allowed a systematic investigation of the NJL model limit, where existing parametrizations could be recovered.

**Table 7. Parameter sets for the chiral quark model with Lorentzian form factor for different values of the  $\alpha$  parameter, when  $-\langle u\bar{u}\rangle^{1/3} = 260$  MeV (for both branches)**

$\alpha$	The lower branch						The higher branch					
	$m_0$ , MeV	$m_{s,0}$ , MeV	$G_S\Lambda^2$	$\phi_{u,d}$ , MeV	$\phi_s$ , MeV	$\Lambda$ , MeV	$m_0$ , MeV	$m_{s,0}$ , MeV	$G_S\Lambda^2$	$\phi_{u,d}$ , MeV	$\phi_s$ , MeV	$\Lambda$ , MeV
5	4.369	139.7	2.745	386.2	536.5	614.76	4.375	129.2	3.379	537.9	651.6	564.79
6	4.378	145.6	2.501	337.2	494.9	648.79	4.384	125.6	3.668	620.4	709.6	558.59
7	4.378	148.7	2.389	317.2	476.7	666.72	4.389	123.8	3.788	661.6	737.8	559.57
8	4.382	150.7	2.318	305.8	465.8	678.13	4.392	122.8	3.849	687.1	754.9	561.56
9	4.379	152.1	2.268	298.4	458.5	686.04	4.394	122.1	3.882	704.4	766.3	563.58
10	4.380	153.2	2.230	293.2	453.2	691.85	4.396	121.5	3.900	717.0	774.4	565.39
12	4.380	154.7	2.177	286.2	445.9	699.79	4.398	120.8	3.917	733.9	785.1	568.36
15	4.381	156.1	2.126	280.2	439.4	706.85	4.400	120.1	3.920	748.8	794.3	571.52
20	4.381	157.5	2.078	274.9	433.5	713.11	4.402	119.5	3.912	761.9	802.2	574.79
30	4.382	158.7	2.032	270.2	428.2	718.63	4.405	118.9	3.894	773.4	808.9	578.09
40	4.382	159.3	2.010	268.2	425.6	721.12	4.406	118.6	3.881	778.6	811.7	579.73
50	4.382	159.6	1.996	266.9	424.2	722.52	4.406	118.5	3.873	781.6	813.4	580.70

**Table 8. Parameter sets for the chiral quark model with Lorentzian form factor for different values of the  $\alpha$  parameter, when  $-\langle u\bar{u}\rangle^{1/3} = 280$  MeV (for both branches)**

$\alpha$	The lower branch						The higher branch					
	$m_0$ , MeV	$m_{s,0}$ , MeV	$G_S\Lambda^2$	$\phi_{u,d}$ , MeV	$\phi_s$ , MeV	$\Lambda$ , MeV	$m_0$ , MeV	$m_{s,0}$ , MeV	$G_S\Lambda^2$	$\phi_{u,d}$ , MeV	$\phi_s$ , MeV	$\Lambda$ , MeV
5	3.522	131.0	2.278	273.2	477.9	758.35	3.520	97.42	5.256	1008	1076	546.27
6	3.523	133.7	2.198	261.8	464.5	779.62	3.522	96.57	5.294	1041	1096	558.38
7	3.523	135.4	2.143	255.1	456.2	792.89	3.525	96.03	5.281	1058	1105	567.40
8	3.523	136.7	2.103	250.7	450.6	801.86	3.524	95.64	5.252	1067	1110	574.24
9	3.526	137.6	2.072	247.6	446.5	808.28	3.526	95.35	5.219	1073	1112	579.55
10	3.525	138.3	2.047	245.3	443.4	813.06	3.532	95.13	5.187	1077	1113	583.78
12	3.524	139.4	2.011	242.1	439.0	819.66	3.527	94.80	5.129	1081	1113	590.05
15	3.527	140.3	1.975	239.1	434.8	825.61	3.528	94.48	5.062	1084	1112	596.21
20	3.524	141.3	1.939	236.5	431.0	830.90	3.530	94.17	4.987	1086	1110	602.20
30	3.525	142.1	1.903	234.0	427.3	835.56	3.533	93.86	4.904	1087	1107	608.00
40	3.526	142.5	1.885	232.9	425.5	837.65	3.535	93.69	4.860	1087	1106	610.81
50	3.526	142.8	1.874	232.2	424.5	838.83	3.537	93.60	4.833	1087	1105	612.47

Table 9. Parameter sets for the chiral quark model with Woods–Saxon form factor for different values of the  $\alpha$  parameter, when  $-\langle u\bar{u}\rangle^{1/3} = 260$  MeV (for both branches)

$\alpha$	The lower branch						The higher branch					
	$m_0$ , MeV	$m_{s,0}$ , MeV	$G_S\Lambda^2$	$\phi_{u,d}$ , MeV	$\phi_s$ , MeV	$\Lambda$ , MeV	$m_0$ , MeV	$m_{s,0}$ , MeV	$G_S\Lambda^2$	$\phi_{u,d}$ , MeV	$\phi_s$ , MeV	$\Lambda$ , MeV
5	4.380	145.0	2.732	356.7	518.6	646.62	4.386	125.4	4.084	672.1	762.0	554.94
6	4.378	147.9	2.560	330.5	493.1	666.14	4.389	123.9	4.108	698.3	775.6	558.34
7	4.378	150.0	2.446	315.1	477.4	678.52	4.391	122.9	4.097	714.3	783.0	561.32
8	4.374	151.6	2.366	305.0	467.0	686.93	4.393	122.2	4.078	725.2	787.9	563.77
9	4.379	152.7	2.307	298.0	459.5	692.98	4.395	121.6	4.058	733.3	791.4	565.79
10	4.380	153.7	2.263	292.9	454.0	697.49	4.396	121.2	4.040	739.6	794.1	567.46
12	4.380	155.0	2.199	286.1	446.5	703.75	4.398	120.6	4.010	748.9	798.2	570.06
15	4.380	156.3	2.141	280.1	439.8	709.43	4.400	120.0	3.979	757.9	802.3	572.76
20	4.381	157.6	2.086	274.8	433.7	714.60	4.402	119.4	3.944	766.8	806.4	575.56
30	4.382	158.7	2.035	270.1	428.2	719.30	4.405	118.9	3.907	775.5	810.6	578.46
40	4.382	159.3	2.011	268.1	425.7	721.50	4.406	118.6	3.889	779.8	812.7	579.95
50	4.382	159.7	1.997	266.8	424.2	722.77	4.400	118.7	3.877	782.4	814.0	580.85

Table 10. Parameter sets for the chiral quark model with Woods–Saxon form factor for different values of the  $\alpha$  parameter, when  $-\langle u\bar{u}\rangle^{1/3} = 280$  MeV (for both branches)

$\alpha$	The lower branch						The higher branch					
	$m_0$ , MeV	$m_{s,0}$ , MeV	$G_S\Lambda^2$	$\phi_{u,d}$ , MeV	$\phi_s$ , MeV	$\Lambda$ , MeV	$m_0$ , MeV	$m_{s,0}$ , MeV	$G_S\Lambda^2$	$\phi_{u,d}$ , MeV	$\phi_s$ , MeV	$\Lambda$ , MeV
2	3.516	123.0	2.658	360.0	586.4	636.21	3.519	98.88	6.018	1223	1324	464.2
5	3.521	132.9	2.378	272.3	481.4	780.90	3.528	96.37	6.024	1155	1209	554.4
6	3.522	134.7	2.280	262.4	468.2	795.37	3.521	95.93	5.824	1138	1185	565.5
7	3.523	136.1	2.208	255.8	459.1	804.73	3.524	95.60	5.664	1127	1169	573.4
8	3.526	137.1	2.154	251.3	452.8	811.16	3.525	95.34	5.538	1118	1156	579.2
9	3.524	137.9	2.112	248.0	448.2	815.77	3.526	95.12	5.440	1112	1148	583.7
10	3.524	138.6	2.080	245.6	444.7	819.24	3.527	94.95	5.362	1108	1141	587.3
12	3.524	139.5	2.033	242.2	439.8	824.08	3.535	94.68	5.247	1102	1132	592.7
15	3.524	140.4	1.989	239.2	435.3	828.51	3.528	94.41	5.135	1097	1123	598.0
20	3.524	141.3	1.947	236.5	431.2	832.57	3.530	94.13	5.026	1093	1116	603.3
30	3.525	142.2	1.906	234.0	427.4	836.31	3.533	93.85	4.920	1089	1110	608.5
40	3.526	142.6	1.887	232.9	425.6	838.08	3.535	93.68	4.869	1088	1107	611.1
50	3.526	142.8	1.875	232.2	424.5	839.12	3.537	93.59	4.839	1088	1106	612.7

Table 11. Parameter sets for the chiral quark model with NJL form factor for different values of the condensate  $-\langle u\bar{u}\rangle^{1/3}$  (for both branches)

$\langle u\bar{u}\rangle^{1/3}$ , MeV	The lower branch						The higher branch					
	$m_0$ , MeV	$m_{s,0}$ , MeV	$G_S\Lambda^2$	$\phi_{u,d}$ , MeV	$\phi_s$ , MeV	$\Lambda$ , MeV	$m_0$ , MeV	$m_{s,0}$ , MeV	$G_S\Lambda^2$	$\phi_{u,d}$ , MeV	$\phi_s$ , MeV	$\Lambda$ , MeV
-280.0	3.5267	143.7	1.8312	229.7	420.6	842.995	3.5212	93.24	4.7187	1085	1200	618.877
-260.0	4.3832	160.9	1.9429	262.3	418.7	727.552	4.4026	117.8	3.8296	792.3	819.0	584.552
-250.8	4.8723	168.0	2.0424	289.5	424.6	672.837	4.9032	133.1	3.3873	657.7	695.2	572.204
-247.5	5.0661	169.9	2.0970	304.0	429.7	652.141	5.0903	139.7	3.2119	606.4	649.5	569.133
-242.4	5.3922	171.3	2.2346	340.1	446.7	616.631	5.4081	152.2	2.8899	515.3	571.8	568.224
-240.8	5.5052	170.4	2.3161	361.4	458.9	602.778	5.5093	157.5	2.7509	477.1	541.0	570.738

We have shown that the instantaneous nonlocal models have an essential problem for the softest form factors, where it is impossible to obtain acceptable values for the chiral condensate. However, for the astrophysical applications this problem could be considered as of minor importance relative to the insights which a systematic variation of the interaction model offers for the better understanding of mechanisms governing the quark matter EoS on a microscopic level.

We show numerically that the Goldberger–Treiman relation and GMOR as low-energy theorems also hold for the nonlocal chiral quark model.

The present approach to nonlocal chiral quark models can be applied subsequently for systematic studies of constraints on the EoS of superdense matter coming from the phenomenology of heavy-ion collisions and compact stars.

**Acknowledgements.** I thank David Blaschke, Norberto Scoccola and Yuri Kalinovsky for the initiation of this work and constructive discussions. I am grateful to A. Dorokhov, O. Teryaev and V. Yudichev for their interest in this work and support during my visit to the JINR, Dubna. This work was supported in part by DFG under grant No. 436 ARM 17/4/05 and by the DAAD partnership program between the Universities of Rostock and Yerevan.

#### REFERENCES

1. Karsch F. hep-lat/0601013.
2. Müller B., Nagle J. L. nucl-th/0602029.
3. Senger P. // Acta Phys. Pol. B. 2006. V. 37. P. 115.
4. Klähn T. et al. nucl-th/0602038.
5. Buballa M. // Phys. Rep. 2005. V. 407. P. 205.
6. Rüter S. B. et al. // Phys. Rev. D. 2005. V. 72. P. 034004.
7. Blaschke D. et al. // Ibid. P. 065020.

8. *Aguilera D. N., Blaschke D., Grigorian H.* // Nucl. Phys. A. 2005. V. 757. P. 527.
9. *Abuki H., Kunihiro T.* // Nucl. Phys. A. 2006. V. 768. P. 118.
10. *Schmidt S. M., Blaschke D., Kalinovsky Y. L.* // Phys. Rev. C. 1994. V. 50. P. 435.
11. *Blaschke D. et al.* // Intern. J. Mod. Phys. A. 2001. V. 16. P. 2267.
12. *Gomez Dumm D. et al.* hep-ph/0512218.
13. *Blaschke D. et al.* // Nucl. Phys. A. 2004. V. 736. P. 203.
14. *Grigorian H., Blaschke D., Aguilera D. N.* // Phys. Rev. C. 2004. V. 69. P. 065802.
15. *Grigorian H., Blaschke D., Voskresensky D.* // Phys. Rev. C. 2005. V. 71. P. 045801.
16. *Popov S., Grigorian H., Blaschke D.* nucl-th/0512098.
17. *Aguilera D. N. et al.* // Phys. Rev. D. 2005. V. 72. P. 034008.
18. *Aguilera D. N., Blaschke D. B.* hep-ph/0512001.
19. *Gocke C. et al.* hep-ph/0104183.
20. *Blaschke D. et al.* // Nucl. Phys. A. 1995. V. 586. P. 711.
21. *Dosch H. G., Narison S.* // Phys. Lett. B. 1998. V. 417. P. 173.
22. *Rehberg P., Klevansky S. P., Hüfner J.* // Phys. Rev. C. 1996. V. 53. P. 410.
23. *Costa P. et al.* // Phys. Rev. D. 2005. V. 71. P. 116002.

Received on April 6, 2006.